A Graphene Oxide Nanosheet Supported NHC–Palladium Complex as a Highly Efficient and Recyclable Suzuki Coupling Catalyst

Yingjie Qian[◇]
Jaeil So[◇]
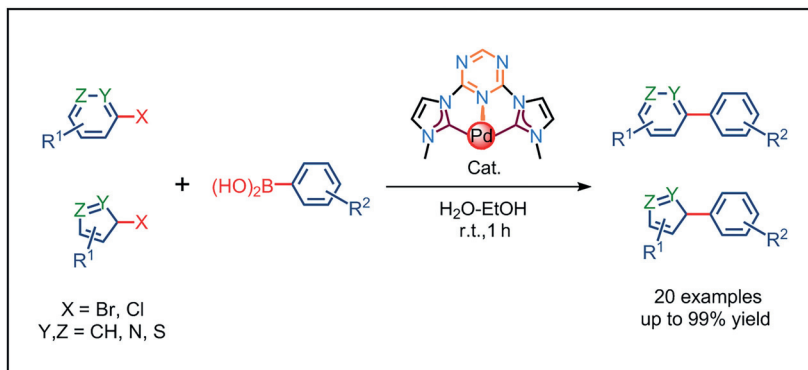Sang-Yung Jung
Sosan Hwang
Myung-Jong Jin* [ID]
Sang Eun Shim* [ID]

Department of Chemistry and Chemical Engineering, Inha University, 100 Inha-ro, Nam-gu, Incheon 22212, South Korea
mjjin@inha.ac.kr
seshim@inha.ac.kr

[◇] These authors contributed equally to this work.

X = Br, Cl
Y,Z = CH, N, S

20 examples
up to 99% yield

Abstract A practical heterogeneous catalyst was prepared by anchoring a triazine-tethered N-heterocyclic carbene (NHC)–palladium complex on the surface of graphene oxide (GO) nanosheets. The immobilized complex was characterized by X-ray photoelectron spectroscopy, field-emission transmission electron microscopy, energy-dispersive X-ray spectroscopy, and surface area analysis. It proved to be a highly active and durable heterogeneous catalyst for Suzuki coupling reactions. At room temperature, the use of this catalyst enabled the preparation of various biaryls and heterobiaryls in short reaction times. The catalytic system could be recycled at least 10 times with almost consistent activity. The results reveal that the stable palladium complex is strongly anchored on the surface of GO nanosheets. Interestingly, an open planar network of the GO nanosheet support plays a role during the catalytic process in enhancing the catalytic activity.

Key words graphene oxide, palladium, immobilization, heterogeneous catalysis, Suzuki coupling

The palladium-catalyzed Suzuki coupling reaction of aryl halides with arylboronic acids represents one of the most important methods for the formation of a carbon–carbon bond.[1] Significant progress has been achieved in this area with a variety of homogeneous palladium catalysts.[2] Although homogeneous catalysts have attractive properties such as high reactivity and selectivity, difficulties are encountered in the separation and recovery of these expensive catalysts from reaction mixtures for reuse.[3] Moreover, homogeneous catalysts tend to lose their activity owing to palladium metal agglomeration and precipitation.[4] Such disadvantages lead to serious economic and environmental concerns in large-scale synthesis. Therefore, the successful development of homogeneous catalysts has been often followed by attempts to immobilize the catalysts on insoluble supports.[5] A desirable method of supporting homogeneous metal complexes involves the formation of a chemical bond between the surface of a solid support and a ligand group in the metal complex. A variety of highly active, heterogeneous palladium catalysts for Suzuki couplings have been developed.[6]

It should be noted that the support may play an important role, affecting the interactions between pendant catalytic sites and substrates, together with the affinity between the support and substrates. The most typical supports include porous inorganic solids such as silica, zeolite, mesoporous materials, and others.[7] However, these materials have high sensitivity towards acid and base conditions.[8] Carbon materials as supports have attracted a fast-growing interest in the recent past due to better corrosion resistance in both alkaline and acidic environments.[9] This is important from a durability point of view, since support corrosion is one of the important factors for the aggregation of catalytic metal particles, which causes considerable loss of catalytic activity. Carbon nanotube supported palladium nanoparticles have been prepared for various catalytic applications.[10]

Graphene oxide (GO) nanosheets, as a form of carbon with a high specific surface area as well as chemical and thermal stability, arise as an excellent candidate as a catalyst support.[11] Homogeneous metal complexes can be easily immobilized through the formation of covalent bonds between the surface of GO nanosheets and silylated ligands, as the nanosheets contain a range of reactive oxygen functional groups on their surface.[12] Another important advantage of GO nanosheet support is concerned with the horizontal open structure. From the point of view of structure openness, GO nanosheets seem to be a unique catalyst support which can lead to enhanced catalytic activity. Although GO nanosheet supported palladium nanoparticles have been developed in recent years,[13] so far there are few reports of the immobilization of homogeneous catalysts on

a GO nanosheet support. Wu and co-workers have reported an efficient GO-supported palladium catalyst (aryldiimine as ligand) for Suzuki coupling reactions.[6a]

It has long been known that N-heterocyclic carbene–palladium (NHC-Pd) complexes act as very effective catalysts in homogeneous couplings.[14] The advantages of adopting NHCs as ligands in Pd-catalyzed couplings are as follows: (1) the strong σ-donating ability of NHCs into the Pd center facilitates the oxidative addition process; (2) the steric bulkiness of NHC substituents renders reductive elimination; and (3) the strong NHC–Pd bond makes it more attractive. Our interest in this area led us to explore NHC-Pd complexes immobilized on commercial GO nanosheets which may have advantages over the homogeneous counterparts. Such heterogeneous catalysts with excellent catalytic performance under mild conditions and long-term durability would be highly desired. Herein, we present a triazine-tethered NHC-Pd heterogeneous catalyst as a useful catalyst for the room temperature Suzuki coupling of aryl halides with arylboronic acids.

As illustrated in Scheme 1, GO nanosheet supported NHC-Pd complex **4** was easily prepared in four steps. Aminopropyl-functionalized GO **1** was simply obtained by refluxing a mixture of GO nanosheets and (3-aminopropyl)triethoxysilane (APTES) in anhydrous toluene. Reaction of **1** with cyanuric chloride in THF gave cyanuric chloride functionalized GO **2**. Subsequently, treatment of **2** with 1-methylimidazole led to the formation of imidazolium-functionalized GO **3**. Complex **4** was obtained by treatment of **3** with Pd(OAc)₂ in THF at 75 °C. Loading amounts of Pd on the surface can be controlled in this step. Complex **4** with a

Pd content of 0.19 mmol/g was prepared for this study; the value was confirmed by inductively coupled plasma atomic optical emission spectrometry (ICP-OES).

To investigate the elemental composition and chemical states of the compounds shown in Scheme 1, X-ray photoelectron spectroscopy (XPS) measurements were performed. As expected, there are only C 1s and O 1s peaks observed in the XPS survey spectrum of GO nanosheets (Figures 1a and S1, see Supporting Information). The N 1s, Si 2p, and Si 2s peaks found in the XPS spectrum of **1** demonstrate the effective silylation of GO nanosheets. Meanwhile, Pd 3d peaks are present at the surface of complex **4**, revealing the successful incorporation of Pd on the GO nanosheets. To further investigate the chemical composition of the surface of the compounds, further study was carried out on the N 1s and Pd 3d XPS spectra.

In the high-resolution N 1s XPS spectrum, **1** displays one peak at 399.8 eV corresponding to primary amine (RNH₂) (Figure 1b).[15] In the expanded XPS spectrum of **2**, the N 1s peaks at 399.46 and 401.1 eV can be assigned to nitrogen in the form of triazine (C=N) and secondary amine (R₂NH), respectively (Figure 1c).[16] In Figure 1d, the N1s XPS spectrum of **3** consists of three peaks at 399.46, 401.1, and 398.9 eV, corresponding to the binding energies of triazine (C=N), R₂NH and N⁺ (imidazole), and R₃N (imidazole), respectively.[17]

After the addition of Pd moieties, the triazine (C=N) and imidazole (R₃N) bands shifted to higher binding energies of 399.66 and 399.09 eV, respectively (Figure 1e). This phenomenon could be explained by donor–acceptor interactions between the nitrogen in ligands and Pd moieties.[18] Moreover, the intensity of the peak at 401.1 eV decreased and the peak at 399.09 eV increased owing to the conversion of N⁺ into R₃N-type nitrogen after anchoring by Pd moieties. Finally, we attempted to determine the oxidation state of Pd in complex **4**. The Pd 3d core level XPS spectrum of complex **4** exhibits main peaks at 337.95 and 343.25 eV, which are assigned to Pd(II) (Figure 1f).[18]

Elemental maps in energy-dispersive X-ray spectroscopy (EDX) of complex **4** show that N and Pd atoms were homogeneously dispersed on the surface of GO nanosheets. The data also clarify that the Pd moieties are anchored on the triazine-tethered NHC ligand (Figure 2).

In addition, structural elucidations of complex **4** and reused catalyst were performed using transmission electron microscopy (TEM) analysis (Figure 3). For complex **4**, it is difficult to find agglomerated Pd nanoparticles, suggesting that most of the Pd moieties are homogeneously dispersed on the surface of the catalyst (Figure 3a,b). TEM images obtained from recovered catalyst **4** show that some Pd nanoparticles are formed at the surface of the catalyst (Figure 3c,d).

The results for N₂ adsorption–desorption containing the Brunauer–Emmett–Teller (BET) surface area (S_{BET}) and the total pore volumes (V_{total}) of GO nanosheets and complex **4**
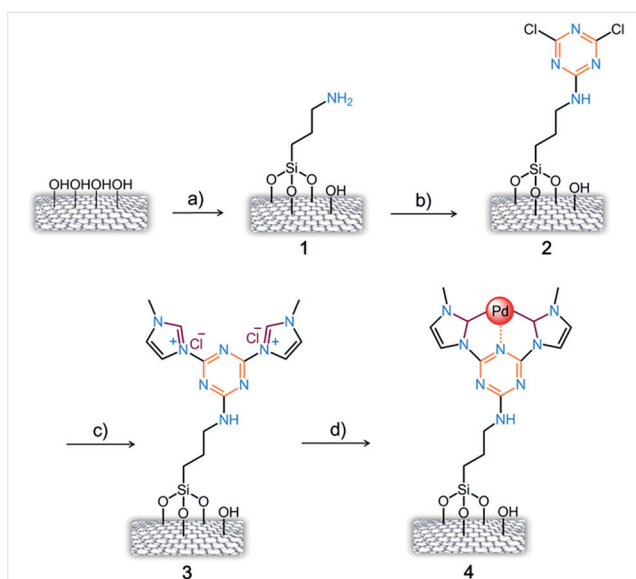
Scheme 1 Synthesis of complex **4**. *Reagents and conditions*: a) APTES, toluene, reflux, 10 h; b) cyanuric chloride, THF, r.t.; c) 1-methylimidazole, 75 °C, 2 h; d) Pd(OAc)₂, THF, 75 °C, 2 h.
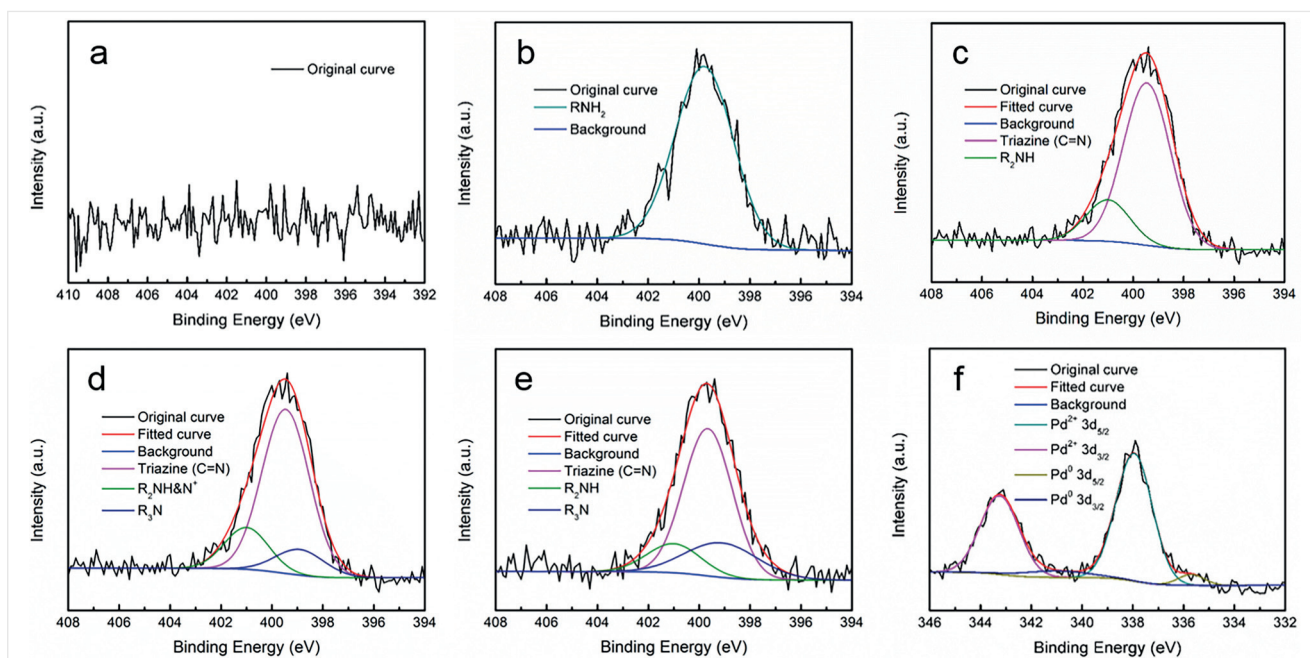
Figure 1 N 1s XPS spectra of (a) GO, (b) **1**, (c) **2**, (d) **3**, and (e) catalyst **4**; (f) Pd 3d XPS spectrum of complex **4**

are summarized in Table S1 (see Supporting Information). The isotherms exhibited type IV hysteresis for GO nanosheets and complex **4** (Figure S2, see Supporting Information). The values for S_{BET} and V_{total} of complex **4** were slightly decreased compared to those of the starting material GO nanosheets.

With complex **4** as the heterogeneous catalyst in hand, we carried out the Suzuki coupling of 4-bromoanisole with phenylboronic acid as a model reaction (see Table S2, Supporting Information). The reaction was initially performed in the presence of 0.2 mol% **4** and 2.0 equivalents of K_2CO_3 in $EtOH/H_2O$, and an excellent yield was obtained within 1 hour at room temperature (entry 1). High catalytic activity was observed with different bases in the presence of 0.1 mol% **4**. K_2CO_3 proved to be the most effective in terms of yield (entries 1–4), whereas other inorganic bases gave moderate yields (entries 5–7) and organic bases were less favorable (entries 8–10). Next, we investigated solvents in the presence of 0.1 mol% **4**. A brief survey revealed that
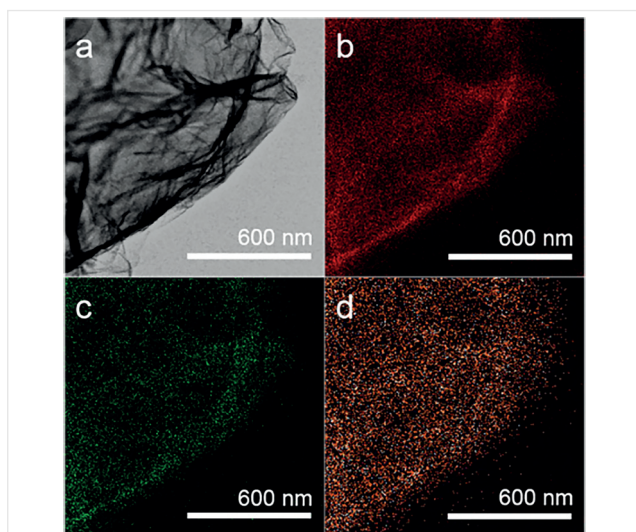
Figure 2 (a) TEM image; EDX mapping images of (b) carbon, (c) nitrogen, and (d) palladium for fresh complex **4**
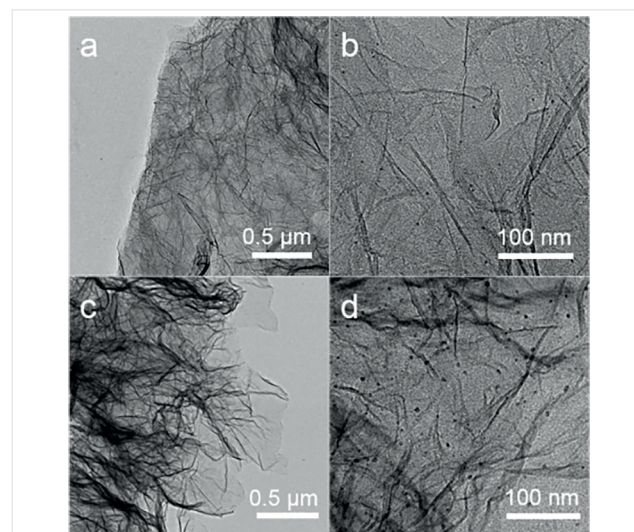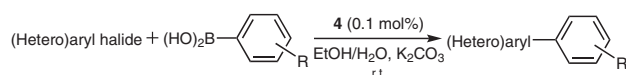

Figure 3 (a) Low-resolution and (b) high-resolution TEM images of fresh complex **4**; (c) low-resolution and (d) high-resolution TEM images of catalyst **4** after 12 runs

EtOH/H$_2$O was the best solvent among those evaluated (entries 11–17).

To further expand the scope of our catalytic system, we next investigated the coupling of various aryl halides with arylboronic acids in the presence of 0.1 mol% **4** at room temperature (Table 1). Bromobenzene and activated aryl bromides such as 1-bromo-2-nitrobenzene and 4-bromobenzonitrile were very well coupled in excellent yields within 0.6 hour (entries 1–3). Deactivated aryl bromides including 2-bromotoluene, 4-bromotoluene, 2-bromoanisole, and 4-bromoanisole were found to furnish the corresponding biaryl products in excellent yields (entries 4–7). Moreover, **4** was efficient for coupling 1-bromonaphthalene and 9-bromoanthracene (entries 8, 9). Importantly, it was also found to be active for unprotected 3-bromoaniline (entry 10). Electron-poor aryl chlorides are far more difficult to activate than aryl bromides.[19] Nevertheless, **4** showed satisfactory efficiency toward 4-chlorobenzonitrile and 1-chloro-2-nitrobenzene at 50 °C for 6 hours (entries 11, 12). Complex **4** was also efficient for the coupling of deactivated aryl halides with electron-rich arylboronic acids at room temperature (entries 13, 14).

Table 1 Suzuki Coupling of Aryl and Heteroaryl Halides with Arylboronic Acids[a]

(Hetero)aryl halide + (HO)$_2$B—⟨aryl⟩—R →[**4** (0.1 mol%); EtOH/H$_2$O, K$_2$CO$_3$, r.t.] (Hetero)aryl—⟨aryl⟩—R

Entry	(Hetero)aryl halide	Product	Time (h)	Yield (%)[b]
1	1-bromo-2-nitrobenzene (O$_2$N, Br)	2-nitrobiphenyl (O$_2$N)	0.5	99
2	bromobenzene (Br)	biphenyl	0.6	99
3	4-bromobenzonitrile (Br—CN)	4-cyanobiphenyl (—CN)	0.5	99
4	4-bromoanisole (Br—OMe)	4-methoxybiphenyl (—OMe)	0.8	99
5	2-bromoanisole (MeO, Br)	2-methoxybiphenyl (MeO)	1	99
6	4-bromotoluene (Br—Me)	4-methylbiphenyl (—Me)	1	99
7	2-bromotoluene (Me, Br)	2-methylbiphenyl (Me)	1	99
8	1-bromonaphthalene (Br)	1-phenylnaphthalene	1	97
9	9-bromoanthracene (Br)	9-phenylanthracene	1	95
10	3-bromoaniline (Br, NH$_2$)	3-aminobiphenyl (NH$_2$)	2	93
11	4-chlorobenzonitrile (Cl—CN)	4-cyanobiphenyl (—CN)	24 / 6[c]	51 / 87[c]
12	1-chloro-2-nitrobenzene (O$_2$N, Cl)	2-nitrobiphenyl (O$_2$N)	24 / 6[c]	65 / 93[c]
13	2-bromotoluene (Me, Br)	2,2′-dimethylbiphenyl (Me, Me)	2	91
14	4-bromotoluene (Br—Me)	4,4′-dimethylbiphenyl (Me—Me)	1	96
15	2-bromo-3-methylpyridine (Me, Br, N)	(Me, N)	4 / 1[c]	83 / 90[c]
16	3-bromopyridine (Br, N)	3-phenylpyridine (N)	4 / 1[c]	87 / 98[c]
17	2-bromopyridine (N, Br)	2-phenylpyridine (N)	4 / 1[c]	91 / 99[c]
18	3-bromothiophene (Br, S)	3-phenylthiophene (S)	4 / 1[c]	89 / 99[c]
19	2-bromothiophene (S, Br)	2-phenylthiophene (S)	4 / 1[c]	87 / 98[c]
20	5-bromothiophene-2-carbaldehyde (S, CHO, Br)	(S, CHO)	2 / 1[c]	87 / 99[c]

[a] Reaction conditions: aryl halide (1.0 mmol), arylboronic acid (1.5 mmol), **4** (0.1 mol%), K$_2$CO$_3$ (2.0 mmol), TBAB (0.5 mmol), H$_2$O (2 mL), EtOH (2 mL), r.t.
[b] GC yield, determined using *n*-dodecane as an internal standard.
[c] The reaction was carried out at 50 °C.

The catalytic system was further extended to the coupling of heteroaryl bromides with phenylboronic acid. The Suzuki coupling of heteroaryl halides is of particular interest to the pharmaceutical industry because many biologically active compounds are accessed through this methodology.[20] Despite their importance, the coupling of heteroaryl bromides remains a challenge, especially at low temperature. It is noteworthy that 3-bromopyridine, 2-bro-

mopyridine, sterically hindered 2-bromo-3-methylpyri-
dine, 3-bromothiophene, 2-bromothiophene, and 5-bro-
mo-2-thiophenecarboxaldehyde could be coupled in good
yield at room temperature, although longer time was re-
quired (Table 1, entries 15–20). In addition, the heteroaryl
halides underwent the coupling at 50 °C to afford the corre-
sponding desired products in high yields in 1 hour. The ex-
cellent catalytic activity of **4** could be explained by the fact
that the triazine-tethered NHC could increase the electron
density of the center Pd, consequently to greatly enhance
the performance of **4**.[14a]

To demonstrate the support effect on catalytic activity,
we compared Pd supported on the most common support
SiO$_2$ (Pd-NHC@SiO$_2$) with **4** (Figure S3, see Supporting In-
formation). Pd-NHC@SiO$_2$ was prepared using the same
method as for catalyst **4**, except for the support. Firstly, we
coupled activated 4-bromobenzonitrile and phenylboronic
acid. After 30 minutes, the reaction showed complete con-
version with **4**, in comparison to 95% with Pd-NHC@SiO$_2$.
Secondly, we selected deactivated 4-bromoanisole as aryl
halide. Within 50 minutes, **4** and Pd-NHC@SiO$_2$ yielded the
coupling product in 99% and 84% yield, respectively. In the
case of 4-bromoanisole, the difference in activity between
the catalysts was much more conspicuous. Finally, we se-
lected 4-chlorobenzonitrile as aryl halide and the reaction
was carried out at 50 °C. After 6 hours, the yields were 87%
and 58% for **4** and Pd-NHC@SiO$_2$, respectively. On the basis
of these findings, we could carefully assert that the struc-
tural openness of GO facilitates the catalysis. It is also note-
worthy that homogeneous triazine-based NHC-Pd catalysts
require somewhat higher temperatures and longer reaction
times to achieve effective couplings[21] and would suffer
from catalyst reuse and recycling problems.

Catalyst reuse is one of the most attractive advantages
of the heterogeneous reaction. The reusability of **4** was in-
vestigated in the reaction of deactivated 4-bromoanisole
with phenylboronic acid. As shown in Figure 4, after 10
times reuse, the excellent catalytic efficiency was still re-
tained without loss of catalytic activity. The catalytic activi-
ty gradually decreased from the 11th run. TEM studies have
confirmed that Pd nanoparticles are formed at the surface
of the GO nanosheets after 12 runs (Figure 3c,d).
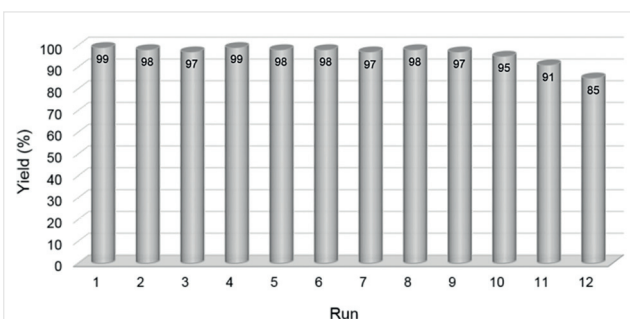
Figure 4 Reuse of catalyst **4** in the Suzuki coupling of 4-bromoanisole with phenylboronic acid

A leaching test was carried out in the coupling of 3-bro-
moaniline with phenylboronic acid. No further reaction
took place after catalyst **4** was removed by filtration (Figure
S4, see Supporting Information). Also, ICP-OES analysis of
the solution indicated that little Pd metal (0.11 ppm)
leached into the solution during the reaction. These results
demonstrated that the high sustainability of the catalyst
could be explained by a strong binding of the triazine-teth-
ered NHC to Pd.

We have compared the results obtained in this work
with various reported heterogeneous catalysts (see Table
S3, Supporting Information), which verified that **4** is highly
efficient in room-temperature Suzuki coupling reactions.
Along with the inherent nature of the free Pd complex, the
excellent reusability and reactivity of **4** could be explained
by the strong binding of triazine-tethered electron-rich
NHCs to the metal center and the structural openness of GO
nanosheets.

In summary, we have developed a highly active, recycla-
ble, GO nanosheet supported, triazine-bridged NHC catalyst
for Suzuki coupling reactions. A wide range of aryl and het-
eroaryl bromides were very well coupled at room tempera-
ture. The catalytic system is also effective for less reactive
aryl chlorides. In particular, the catalytic activity remained
high after several reuses. Along with the inherent nature of
the free Pd complex, the high efficiency appears to be due
to the good stability of the catalytically active Pd species on
GO nanosheets. The simple preparation of **4**, in combina-
tion with its high catalytic activity and recyclability, may
hopefully stimulate future research in the field of heteroge-
neous catalysis. Further studies of other coupling reactions
are currently in progress.

All chemicals are commercially available and were used as purchased
without any further purification. Graphene oxide (GO) was obtained
from Anstrong Materials. All other chemicals were purchased from
Sigma Aldrich, TCI, and Alfa Aesar. X-ray photoelectron spectroscopy
(XPS) data were collected using an ESCA 2000 photoelectron spec-
trometer (Thermo Scientific) with monochromated Al Kα radiation
($h\nu$ = 1486.6 eV). NMR spectra were recorded on a Bruker DIGITAL
AVANCE III (400 MHz) spectrometer. Field-emission transmission
electron microscopy (FE-TEM) images were acquired by employing a
JEOL JEM-2100F microscope. The specific surface area and pore size
distribution of the catalyst were investigated by measuring the nitro-
gen adsorption and desorption isotherms at 77 K on a BELSORP-MAX
system (BEL, Japan). GC/GC-MS analyses were performed on an Agi-
lent 6890N GC coupled to an Agilent 5975 Network Mass Selective
Detector.

Aminopropyl-Functionalized GO 1

GO (200 mg) was dispersed in anhydrous toluene (100 mL) under son-
ication for 1 h. (3-Aminopropyl)triethoxysilane (APTES) (0.05 mL,
0.21 mmol) was dropwise added into the GO suspension. The mixture
was stirred under reflux for 10 h. After allowing the mixture to cool to
r.t., the mixture was filtered, washed with methylene chloride, and
dried at 75 °C under vacuum to give **1**.

Cyanuric Chloride Functionalized GO 2

A solution of GO **1** (100 mg) in THF (30 mL) was sonicated for 30 min at r.t.. To this solution, cyanuric chloride (100 mg, 0.54 mmol) and tributylamine (112 mg, 0.6 mmol) were added at 0 °C. After stirring for 10 min at 0 °C, the solution was warmed to r.t. over 20 min. The resulting mixture was filtered, washed with methylene chloride, and dried at 75 °C under vacuum to give **2**.

Imidazolium-Functionalized GO 3

After adding **2** (50 mg) to 1-methylimidazole (10 mL), the mixture was sonicated for 30 min. Then, the mixture was stirred at 75 °C for 2 h. The resulting mixture was cooled to r.t., filtered, washed with Et$_2$O, and dried at 75 °C under vacuum to give **3**.

GO Nanosheet Supported NHC-Pd Complex 4

After adding **3** (50 mg) to THF (15 mL), the mixture was sonicated for 30 min. Pd(OAc)$_2$ (2.5 mg, 0.011 mmol) was added to the mixture which was then stirred at 75 °C for 2 h. The resulting mixture was cooled to r.t., filtered, washed with methylene chloride, and dried at 75 °C under vacuum to give **4**. The Pd content of 0.19 mmol/g was measured by ICP-OES.

Pd-Anchored SiO$_2$ (Pd-NHC@SiO$_2$)

According to the same procedure as described above, Pd-NHC@SiO$_2$ was prepared with SiO$_2$ support. The Pd content of 0.175 mmol/g was measured by ICP-OES.

Suzuki Coupling Reaction; General Procedure

Aryl halide (1.0 mmol), arylboronic acid (1.5 mmol), TBAB (0.5 mmol), K$_2$CO$_3$ (2.0 mmol), and catalyst **4** (0.1 mol%) were mixed in H$_2$O/EtOH (2 mL/2 mL). The mixture was stirred at r.t. in an air atmosphere. The reaction progress was monitored by GC. After reaction completion, the mixture was diluted with H$_2$O and Et$_2$O. The organic layer was separated from mixture, dried over anhydrous MgSO$_4$, and concentrated under reduced pressure. The crude reaction product was purified using column chromatography on silica gel to afford the corresponding product in good yield. In the recycling experiment, after the completion of the reaction, catalyst was separated from the reaction mixture by filtration. The separated catalyst was washed with H$_2$O, EtOH, and Et$_2$O. It was directly used in the next run under the same reaction conditions.

Funding Information

Supporting Information

Supporting information for this article is available online at https://doi.org/10.1055/s-0037-1611726.

References

(1) Seechurn, C. C. C. J.; Kitching, M. O.; Colacot, T. J.; Snieckus, V. *Angew. Chem. Int. Ed.* **2012**, *51*, 5062.

(2) (a) Lee, J. Y.; Ghosh, D.; Lee, J. Y.; Wu, S. S.; Hu, C. H.; Liu, S. D.; Lee, H. M. *Organometallics* **2014**, *33*, 6481. (b) Lee, D.-H.; Jin, M.-J. *Org. Lett.* **2011**, *13*, 252.

(3) Welch, C. J.; Albaneze-Walker, J.; Leonard, W. R.; Biba, M.; DaSilva, J.; Henderson, D.; Laing, B.; Mathre, D. J.; Spencer, S.; Bu, X. D.; Wang, T. B. *Org. Process Res. Dev.* **2005**, *9*, 198.

(4) Astruc, D. *Inorg. Chem.* **2007**, *46*, 1884.

(5) Jin, M.-J.; Lee, D.-H. *Angew. Chem. Int. Ed.* **2010**, *122*, 1137.

(6) (a) Xue, Z. Q.; Huang, P. P.; Li, T. S.; Qin, P. X.; Xiao, D.; Liu, M. H.; Chen, P. L.; Wu, Y. J. *Nanoscale* **2017**, *9*, 781. (b) Yuan, D. Z.; Chen, L.; Yuan, L. G.; Liao, S. J.; Yang, M. M.; Zhang, Q. H. *Chem. Eng. J.* **2016**, *287*, 241.

(7) Veerakumar, P.; Thanasekaran, P.; Lu, K. L.; Liu, S. B.; Rajagopal, S. *ACS Sustainable Chem. Eng.* **2017**, *5*, 6357.

(8) Lowe, B. M.; Skylaris, C. K.; Green, N. G. *J. Colloid Interface Sci.* **2015**, *451*, 231.

(9) Julkapli, N. M.; Bagheri, S. *Int. J. Hydrogen Energy* **2015**, *40*, 948.

(10) (a) Giacalone, F.; Campisciano, V.; Calabrese, C.; Parola, V. L.; Syrgiannis, Z.; Prato, M.; Gruttadauria, M. *ACS Nano* **2016**, *10*, 4627. (b) Jawale, D. V.; Gravel, E.; Boudet, C.; Shah, N.; Geertsen, V.; Li, H. Y.; Namboothiri, I. N. N.; Doris, E. *Catal. Sci. Technol.* **2015**, *5*, 2388. (c) Song, H. Q.; Zhu, Q.; Zheng, X. J.; Chen, X. G. *J. Mater. Chem. A* **2015**, *3*, 10368.

(11) (a) Chen, X. M.; Wu, G. H.; Chen, J. M.; Chen, X.; Xie, Z. X.; Wang, X. R. *J. Am. Chem. Soc.* **2011**, *133*, 3693. (b) Fan, X. B.; Zhang, G. L.; Zhang, F. B. *Chem. Soc. Rev.* **2015**, *44*, 3023.

(12) Baran, T.; Sargin, I.; Kaya, M.; Mentes, A.; Ceter, T. *J. Colloid Interface Sci.* **2017**, *486*, 194.

(13) (a) Scheuermann, G. M.; Rumi, L.; Steurer, P.; Bannwarth, W.; Mulhaupt, R. *J. Am. Chem. Soc.* **2009**, *131*, 8262. (b) Yamamoto, S. I.; Kinoshita, H.; Hashimoto, H.; Nishina, Y. *Nanoscale* **2014**, *6*, 6501. (c) Santra, S.; Hota, P. K.; Bhattacharyya, R.; Bera, P.; Ghosh, P.; Mandal, S. K. *ACS Catal.* **2013**, *3*, 2776.

(14) (a) Valente, C.; Calimsiz, S.; Hoi, K. H.; Mallik, D.; Sayah, M.; Organ, M. G. *Angew. Chem. Int. Ed.* **2012**, *51*, 3314. (b) Hopkinson, M. N.; Richter, C.; Schedler, M.; Glorius, F. *Nature* **2014**, *510*, 485.

(15) Xiao, L. H.; Zheng, X.; Zhao, T. Y.; Sun, L. Y.; Liu, F. Q.; Gao, G.; Dong, A. *Colloid Polym. Sci.* **2013**, *291*, 2359.

(16) Fu, Y. S.; Zhu, J. W.; Hu, C.; Wu, X. D.; Wang, X. *Nanoscale* **2014**, *6*, 12555.

(17) Liu, W. S.; Koh, K. L.; Lu, J. L.; Yang, L. P.; Phua, S.; Kong, J. H.; Chen, Z.; Lu, X. H. *J. Mater. Chem.* **2012**, *22*, 18395.

(18) Zhao, Q. S.; Zhu, Y. Z.; Sun, Z.; Li, Y.; Zhang, G. L.; Zhang, F. B.; Fan, X. B. *J. Mater. Chem. A* **2015**, *3*, 2609.

(19) Alonso, F.; Beletskaya, I. P.; Yus, M. *Tetrahedron* **2008**, *64*, 3047.

(20) Tyrrell, E.; Brookes, P. *Synthesis* **2003**, 469.

(21) Gao, C.; Zhou, H. J.; Wei, S. P.; Zhao, Y. S.; You, J. S.; Gao, G. *Chem. Commun.* **2013**, *49*, 1127.